Environ Sci Pollut Res (2010) 17:798–806
DOI 10.1007/s11356-009-0153-1

AREA 7.2 • INTERACTIONS OF CHEMICALS • RESEARCH ARTICLE

Interaction of nano-TiO_2 with lysozyme: insights into the enzyme toxicity of nanosized particles

Zhen Xu · Xi-Wei Liu · Yin-Sheng Ma · Hong-Wen Gao

Received: 3 March 2009 / Accepted: 1 April 2009 / Published online: 24 April 2009
© Springer-Verlag 2009

Abstract
Background, aim, and scope Nanomaterials have been used increasingly in industrial production and daily life, but their human exposure may cause health risks. The interactions of nanomaterial with functional biomolecules are often applied as a precondition for its cytotoxicity and organ toxicity where various proteins have been investigated in the past years. In the present study, nano-TiO_2 was selected as the representative of nanomaterials and lysozyme as a representative for enzymes. By investigating their interaction by various instrumentations, the objective is to identify the action sites and types, estimate the effect on the enzyme structure and activity, and reveal the toxicity mechanism of nanomaterial.
Materials and methods Laboratory-scale experiments were carried out to investigate the interactions of nano-TiO_2 with lysozyme. The interaction of nano-TiO_2 particles with lysozyme has been studied in the analogous physiological media in detail by UV spectrometry, fluorophotometry, circular dichroism (CD), scanning electron microscope, ζ-potential, and laser particle size.
Results The interaction accorded with the Langmuir isothermal adsorption and the saturation number of lysozyme is determined to be 580 per nano-TiO_2 particle (60 nm of size) with 4.7×10^6 M^{-1} of the stability constant in the physiological media. The acidity and ion strength of the media obviously affected the binding of lysozyme. The warping and deformation of the lysozyme bridging were demonstrated by the conversion of its spatial structure from α-helix into a β-sheet, measured by CD. In the presence of nano-TiO_2, the bacteriolysis activity of lysozyme was subjected to an obvious inhibition.
Discussion The two-step binding model of lysozyme was proposed, in which lysozyme was adsorbed on nano-TiO_2 particle surface by electrostatic interaction and then the hydrogen bond (N–H···O and O–H···O) formed between nano-TiO_2 particle and polar side groups of lysozyme. The adsorption of lysozyme obeyed the Langmuir isothermal model. The binding of lysozyme is dependent on the acidity and ion strength of the media. The bigger TiO_2 aggregate was formed in the presence of lysozyme where lysozyme may bridge between nano-TiO_2 particles. The coexistence of nano-TiO_2 particles resulted in the transition of lysozyme conformation from an α-helix into a β-sheet and a substantial inactivation of lysozyme. The β-sheet can induce the formation of amyloid fibrils, a process which plays a major role in pathology.
Conclusions Lysozyme was adsorbed on the nano-TiO_2 particle surface via electrostatic attraction and hydrogen bonds, and they also bridged among global nano-TiO_2 particles to form the colloidal particles. As a reasonable deduction of this study, nano-TiO_2 might have some toxic impacts on biomolecules. Our data suggest that careful

Responsible editor: Stefan Trapp

Electronic supplementary material The online version of this article (doi:10.1007/s11356-009-0153-1) contains supplementary material, which is available to authorized users.

Z. Xu · H.-W. Gao (✉)
State Key Laboratory of Pollution Control and Resource Reuse,
College of Environmental Science and Engineering,
Tongji University,
Shanghai 200092, China
e-mail: emsl@mail.tongji.edu.cn

X.-W. Liu
Department of Chemistry, Tongji University,
Shanghai 200092, China

Y.-S. Ma
Environmental Engineering College, Nanjing Forestry University,
Nanjing 210037, China

attention be paid to the interaction of protein and nanomaterials. This could contribute to nanomaterial toxicity assessment.

Recommendations and perspectives Our results strongly suggest that nano-TiO_2 has an obvious impact on biomolecules. Our data suggest that more attention should be paid to the potential toxicity of nano-TiO_2 on biomolecules. Further research into the toxicity of nanosized particles needs to be carried out prior to their cell toxicity and tissue toxicity. These investigations might serve as the basis for determining the toxicity and application of nanomaterials.

Keywords Adsorption · Lysozyme · Nano-TiO_2 · Nanoscale titanium dioxide · Noncovalent interaction

1 Background, aim, and scope

More and more nanomaterials are being used in industrial production and daily life because of their unique characteristics (Hund-Rinke and Simon 2006; Stone et al. 2007). For example, some of them are added in sunscreens to absorb UV light and in toothpaste and paints to give them a white color which lasts for years. Some are used in the electronics industry. Besides, there are also many applications in medicine, sporting equipment, cosmetics, coatings, fuel cells, and other industries (Wang et al. 2007; Lovern et al. 2007; Lu et al. 2008; Chen et al. 2005). Nowadays, some nanomaterials are being tried as drug delivery products, and they can help to diagnose diseases as quantum dots that can allow the visualization of cancer cells within the body. With an increasing use of nanomaterials, their human exposure is inevitable. It is important to consider the hazards of these materials. The particle size of nanomaterial is smaller than cells and cellular organelles. It may penetrate these basic blocks, produce physical damage, or induce harmful inflammatory responses. The oxidative stress of nanoparticles can damage lipids, carbohydrates, proteins, and DNA in which lipid peroxidation is considered most dangerous, leading to alterations in cell membrane properties (Buzea et al. 2006; Heinlaan et al. 2008). A large amount of epidemiological and experimental studies indicate that ultrafine particles have close relationships to many respiratory and cardiovascular diseases, such as pneumonia, lung cancer, arteriosclerosis, and myocardial infarction (Zhu et al. 2008). Recent studies have shown that nanomaterials can cause genotoxicity and cytotoxicity in cultured human cells. There is evidence that nano-TiO_2 can cause inflammation, fibrosis, pulmonary damage, and even DNA damage (Donaldson et al. 2001; Dunford et al. 1997; Fenech 2000). As an example, the goblet cell hyperplasia and Muc 5ac expression were induced in rats after a single intratracheal instillation of nano-TiO_2. Nano-TiO_2 might enter the human stratum corneum and interact with the immune system. Oxidative DNA damage and increases in the level of cellular nitric oxide were also observed in human bronchial epithelial cells after exposure to nano-TiO_2 (Wang et al. 2007; Zhu et al. 2008).

Lysozyme, which occurs naturally in egg white, human tears, saliva, and other body fluids, is capable of destroying the cell walls of certain bacteria and thereby acting as a mild antiseptic, a feature that was discovered serendipitously in 1922 by Alexander Fleming. It has been extensively used as a model enzyme in studies on enzymology, molecular biology, genetics, protein chemistry, and immunology (Van Dael 1998). The structure of lysozyme which contains a single chain of 129 amino acid residues was characterized by X-ray analysis. Under normal physiological conditions, lysozyme is folded into a compact, globular structure with a long cleft on the surface. It has many pharmacological functions, such as antiseptic, antiphlogistic, repercussive, antiviral, and antineoplastic actions, as it is effective against gram-positive bacterial cells by hydrolyzing their polysaccharide components. It also improves the human blood circulation and enhances the human immunity (Chen et al. 2008). It is highly expressed in hematopoietic cells where lysozyme is found in granulocytes, monocytes, and macrophages as well as in the bone marrow precursors (Merlini and Bellotti 2005).

The interactions of nanomaterial, e.g., often nano-TiO_2, with the functional biomolecules, e.g., protein, enzyme, DNA, are often applied considering the precondition of its cytotoxicity and organ toxicity, actions where various proteins have been investigated in the past years, e.g., fibrinogen, human serum albumin, and lysine (Gao et al. 2008; Roddick-Lanzilotta et al. 1998; Sela et al. 2007; Voros 2004; Chen et al. 1999). Giacomelli et al. (1997), for example, reported that the structural effects were related to the different conformational states that bovine serum albumin (BSA) molecules adopted with changes in pH, whereas electrostatic effects were analyzed assuming that BSA molecules behaved as soft particles. Voros's (2004) measurements indicated that water and solvent molecules not only influence the 3D structure of proteins in solution, but also play a crucial role in their adsorption onto nanomaterial surfaces. Turkan Kopac and Yener (2008) investigated the effects of pH and temperature on the equilibrium and the kinetics of BSA adsorption onto nano-TiO_2. Chen et al. (1999) reported that the electrostatic interactions are the main mechanism controlling the adsorption of fibrinogen to TiO_2. In this work, nano-TiO_2 was selected as being representative of nanomaterials and lysozyme as representative for enzymes. By investigating their interaction using various instruments, the objective is to identify the action sites and types and to estimate the effect on the enzyme structure and activity.

2 Materials and methods

2.1 Instruments and materials

The absorption spectra of all liquids/solutions were recorded with a Model Lambda-25 Spectrometer (Perkin-Elmer, USA) equipped with a thermostatic cell holder attachment to link with a Model TS-030 Water-Circulated Thermostatic Oven (Yiheng Sci. Technol., Shanghai, China). A Model J-715 CD Spectropolarimeter (Jasco Instrum., Japan) was used to measure the lysozyme conformation. The fluorescence spectra of solutions were recorded with a Model F-4500 Fluorescence Spectrophotometer (Hitachi, Japan). The ζ-potential measurement was carried out on a Model Zetasizer Nano ζ-Potential Analyzer (Malvern Instruments, UK). A Model LS230 Particle Size Analyzer (Beckman Coulter, USA) with a Model LFC-101 Laser Channel (Ankersmid, Holland) was used to measure the size distribution of the particles by using the LS v3.29 operation software. A scanning electron microscope (SEM; Model Quanta 200 FEG, FEI, USA) was used to measure the size and shape of the nano-TiO_2 and nano-TiO_2–lysozyme particles. A Model TG16-WS Centrifuge (Hunan Xiangyi Instruments, China) was used to separate the particles.

Nano-TiO_2 (2.00 mg/L; P25, Degussa, average particle size 21 nm, Germany) was used without further modification (Oliva et al. 2003). It was suspended in deionized water and mixed ultrasonically for 10 min before use. Egg white lysozyme (2.00 mg/mL; Shanghai Chemical Reagents, China Med. Group) was dissolved in deionized water and stored at less than 4°C. A series of Britton–Robinson (B-R) buffer solutions, pH 4.0, 4.5, 5.0, 5.5, 6.0, 6.5, 7.0, 7.4, 8.0, and 8.4, was prepared to adjust the acidity of the solution. An electrolyte solution (1.5 M NaCl) was prepared to adjust the ionic strength of the solution. A set of commercial reagent packets (Jiancheng Bioengineering Institute, Nanjing, China) with 4 U of *Micrococus lysodeikticu* bacterial powder (5 mg/U) as substrate and one bottle of the bacterial powder's solvent (100 mL) was used for the determination of lysozyme activity. The bacterial powder's solvent is the pH 6.2 phosphate buffer consisting of 1.17% NaH_2PO_4, 0.786% Na_2HPO_4, and 0.0392% ethylenediaminetetraacetic acid.

2.2 UV photometric determination of the nano-TiO_2–lysozyme interaction

All studies were carried out in 10-mL calibrated flasks containing 0.14, 0.28, 0.42, 0.56, 0.69, 0.83, 0.97, 1.11, 1.25, 1.39, 1.74, and 2.08 μM lysozyme, 2.0 mL of pH 7.4 B-R buffer, 1.0 mL of 1.5 M NaCl, and a known volume of 300 mg/L nano-TiO_2 suspension. Each suspension was diluted to 10.0 mL with deionized water and mixed thoroughly. After 10 min (Fig. S1 of the Electronic supplementary material), the solid with adsorbed lysozyme was separated by centrifugation of a suspension at 12,000 rpm (twice, 10 min). The absorbance of the supernatant was measured at 280 nm against water by UV–Vis spectrophotometry. Simultaneously, a reagent blank without lysozyme was performed according to the same procedure.

With the above procedures, a series of suspensions was prepared, initially containing 0, 50, 100, 150, 200, 250, and 300 mg/L lysozyme, 140 mg/L nano-TiO_2, 2.0 mL of pH 7.4 B-R buffer, and1.0 mL of 1.5 M NaCl. Each suspension was diluted to 10.0 mL with deionized water and mixed thoroughly. After 10 min, the absorption spectra of the suspension were measured between 480 and 600 nm against water by spectrophotometry.

2.3 Particle size and ζ-potential measurement

With the above procedures, a series of suspensions was prepared, initially containing 0, 0.42, 0.97, 1.39, and 2.08 μM lysozyme, 140 mg/L nano-TiO_2, 2.0 mL of pH 7.4 B-R buffer, and1.0 mL of 1.5 M NaCl. Each suspension was diluted to 10.0 mL with deionized water and mixed thoroughly. After 10 min, the size distribution of the particles in the suspension was measured by a particle size analyzer. In addition, their ζ-potentials were measured by a ζ-potential analyzer.

2.4 Fluorescence measurement

Studies were carried out in 10-mL calibrated flasks containing a known volume of 0.694 μM lysozyme, 2.0 mL of pH 7.4B-R buffer, 1.0 mL of 1.5 M NaCl, and 0, 2, 4, 6, 8, 10, 15, 20, 25, 30, 40, 50, 60, 80, and 100 mg/L nano-TiO_2 suspension. The suspension was diluted to 10.0 mL with deionized water and mixed thoroughly. After 10 min, the fluorescence spectrum of each suspension was measured, where the excitation wavelength was at 280 nm and the emission wavelength was between 300 and 450 nm (both using 5 nm of slit width). Besides, the solid with adsorbed lysozyme was separated according to the method noted above and then the fluorescence spectrum of the supernatant was determined. Simultaneously, a reagent blank without lysozyme was performed according to the same procedure.

2.5 CD measurement

CD spectra were recorded over the range 190–250 nm on a spectropolarimeter. One milliliter of pH 7.4 B-R buffer was mixed with 1.39 μM lysozyme and 0, 5, 20, and 40 mg/L nano-TiO_2 were added, respectively. Each suspension was

allowed to equilibrate for 15 min, and CD spectra were measured in a 0.1-cm light path cell. The mean residue ellipticity (MRE) was calculated. Simultaneously, the reagent blank without lysozyme was measured for correcting the MRE of lysozyme. Three replicate measurements of each were performed. The relative contents of secondary structure forms of lysozyme: α-helix, β-pleated sheet, β-turn, and random coil were calculated.

2.6 Assay of lysozyme activity

The conventional turbidimetric method (Lee and Yang 2002) is used to determine the lysozyme activity in the presence of nano-TiO_2 at pH 7.4. According to the user manual provided by the manufacturer, both the *M. lysodeikticu* bacterial powder (5 mg) and the bacterial powder's solvent (20.0 mL) were mixed to prepare the bacterial suspension (0.25 mg/mL). A standard lysozyme solution (0.010 mg/L) and a sample lysozyme solution with B-R were prepared and placed in a constant temperature water bath at 37°C for more than 5 min; 0.2 mL of each was placed into a colorimetric cell and then 2.0 mL of the bacterial suspension was added immediately. Five and 125 s later, the transmittancies (T_{S0} and T_{S2} for the standard lysozyme and T_0 and T_2 for the work lysozyme) of the suspensions were measured at 530 nm against water. The lysozyme activity (A_{lys}) was calculated by the relation: $A_{lys} = \frac{T_2 - T_0}{T_{S2} - T_{S0}} \times 10 \times 20$.

3 Results and discussion

3.1 Interaction of lysozyme with nano-TiO_2 particles

The light absorption of the lysozyme–nano-TiO_2 suspension is shown in Fig. 1a. The absorbance (A) of the liquid increases with an increase in the lysozyme concentration from 0 to 300 mg/L. The light absorption model: $A = \varphi\varepsilon^{-2}\lambda^{-\sqrt{\varepsilon}}$ (Gao 1999) was used to analyze the variation of the suspending particles where λ is the measurement wavelength, φ the particle number factor being proportional to the number of suspending particles, and ε the particle size factor being inversely proportional to the diameter of suspending particle. From the curves in Fig. 1b, c, plot log$A$ vs. logλ are well linear. Both φ and ε decrease with an increase of lysozyme concentration. Thus, the number of suspending particles decreased and the diameter became larger with increasing lysozyme. This indicated that lysozyme bound to the TiO_2 surface and then caused the self-aggregation of TiO_2 particles. Especially when the mass ratio of lysozyme to TiO_2 is between 0.7 and 1.4, changes of both φ and ε are most obvious. A little amount of lysozyme aggregated on nano-TiO_2 particles when

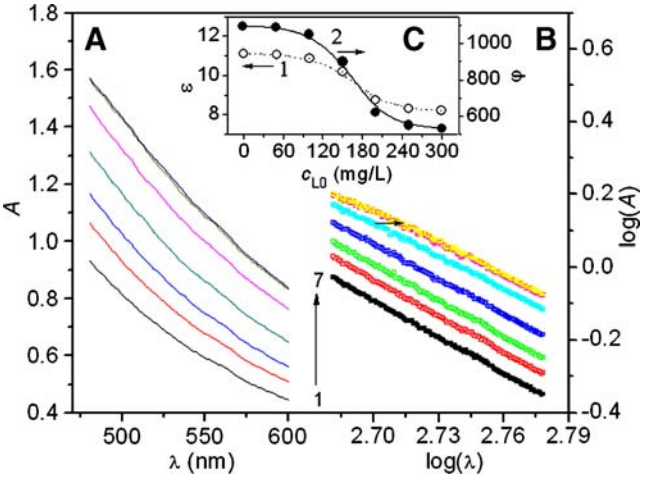

Fig. 1 **a** Absorbance spectra of the nano-TiO_2–lysozyme liquids containing 140 mg/L TiO_2, 0.15 M NaCl, and lysozyme from 0 to 300 mg/L (from curve *1* to *7*) at pH 7.4, all measured against the reagent blank; **b** plots log$A$ vs. logλ of the above liquids; **c** variations of ε (*curve 1*) and φ (*curve 2*) of the suspending particles with the initial concentration (c_{L0}) of lysozyme

the ratio is less than 0.7, but the aggregation of lysozyme approaches adsorption saturation when the ratio is more than 1.4. From Fig. 2, the binding number (γ) of lysozyme increases when the lysozyme increases from 0 to 1.74 μM. The adsorption reaches a plateau when the lysozyme concentration (c_{L0}) is more than 2.08 μM. Thus, the interaction of lysozyme with nano-TiO_2 may be a surface adsorption process and the Langmuir isothermal equation, $\frac{1}{\gamma} = \frac{1}{N} + \frac{1}{KNc_L}$, (Li et al. 2007) ($N$ is the saturation number of lysozyme and K is the stability constant) was used to fit the data. Plots γ^{-1} vs. c_L^{-1} is highly linear (see Fig. 2)

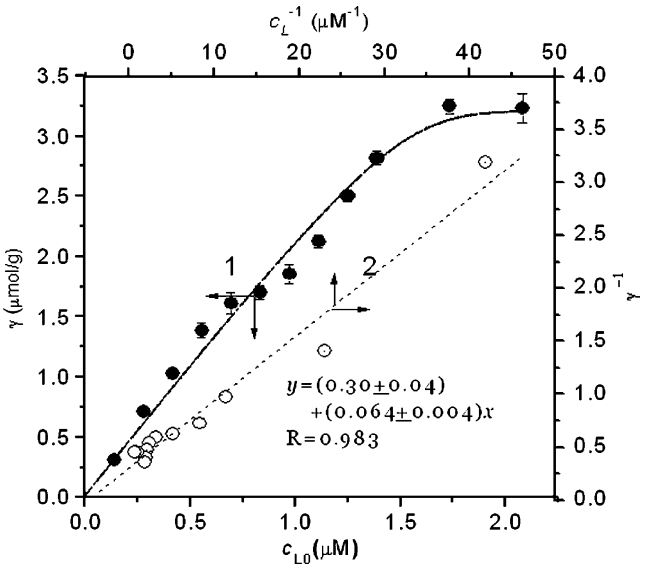

Fig. 2 *1* Variation of γ of the nano-TiO_2–lysozyme suspensions containing 140 mg/L TiO_2, 0.15 M NaCl, and lysozyme from 0 to 2.08 μM at pH 7.4; *2* plots γ^{-1} vs. c_L^{-1} of the above liquids

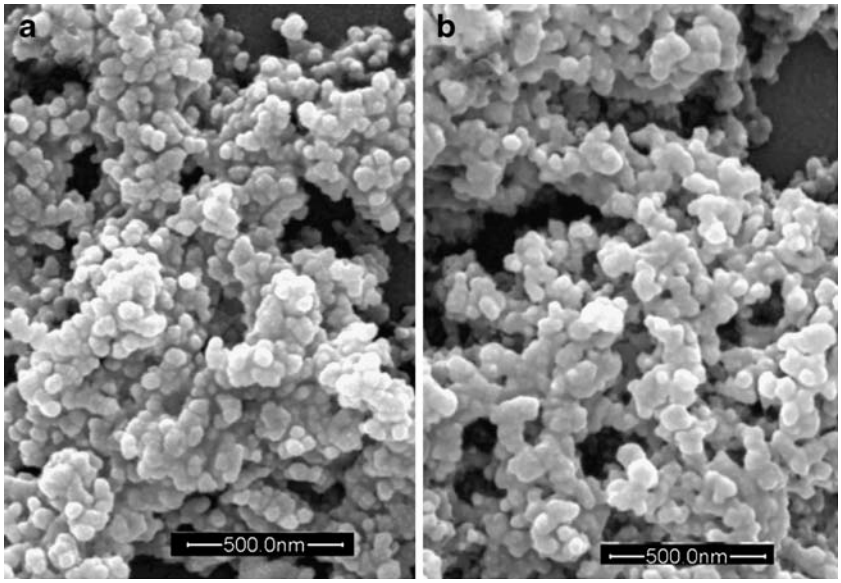

Fig. 3 SEM images of nano-TiO_2 (140 mg/L) (**a**) and nano-TiO_2 (140 mg/L)–lysozyme (300 mg/L) (**b**) particles

and the interaction obeyed the chemical adsorption isotherm in a monolayer. N was calculated to be 3.5± 0.5 μmol/g, i.e., 580±70 moles of lysozyme per mole of nano-TiO_2 particles calculated according to 60±10 nm of the particle size (Fig. 3a). Thus, one nano-TiO_2 particle can adsorb 580 saturated lysozyme molecules on its surface. The K value was calculated to be $(4.7\pm0.3)\times10^6$ M^{-1} and it is higher than that of 2′,4′,5′,7′-tetrabromo-4,5,6,7-tetrachlorofluorescein binding to protein (Gao et al. 2006) and close to that of reactive brilliant red X-3B binding to lysozyme (Chen et al. 2008). Similar to the small molecule–protein interaction, the interaction of lysozyme with nano-TiO_2 particle may be mainly due to the noncovalent combination of the electrostatic interaction with hydrogen bonds.

3.2 Effect of lysozyme on surface potential and size of particles

From Fig. 4a, the ζ-potential of nano-TiO_2 particles is −49 mV, but it increases up to +0.19 mV with an increase of the lysozyme concentration from 0 to 2.08 μM. Obviously, nano-TiO_2 particle surfaces carry lots of negative charges because its isoelectric point is at pH 6 (Oliva et al. 2003). In contrast, lysozyme with 27 basic amino acid residues carries lots of positive charges in a neutral media (the isoelectric point is at pH 11; Liu et al. 1995) (Fig. 5a). At first, the adsorption of lysozyme occurred by the electrostatic attraction when lysozyme is mixed into nano-TiO_2 particle suspension. When the distance between lysozyme and TiO_2 is short enough, the

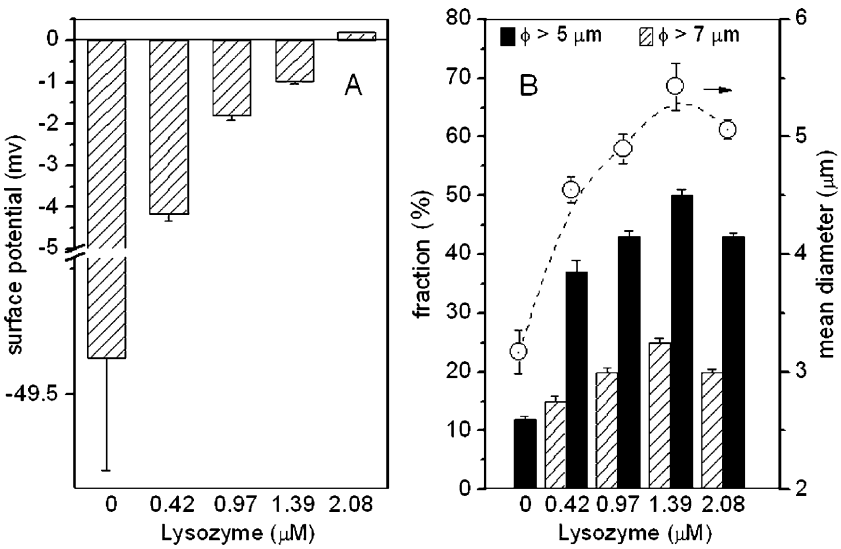

Fig. 4 Variations of surface potential (**a**) and size (**b**) of the suspending particles in the suspensions with the lysozyme concentration (c_{L0}) where all suspensions contained 140 mg/L nano-TiO_2 at pH 7.4 in 0.15 M NaCl

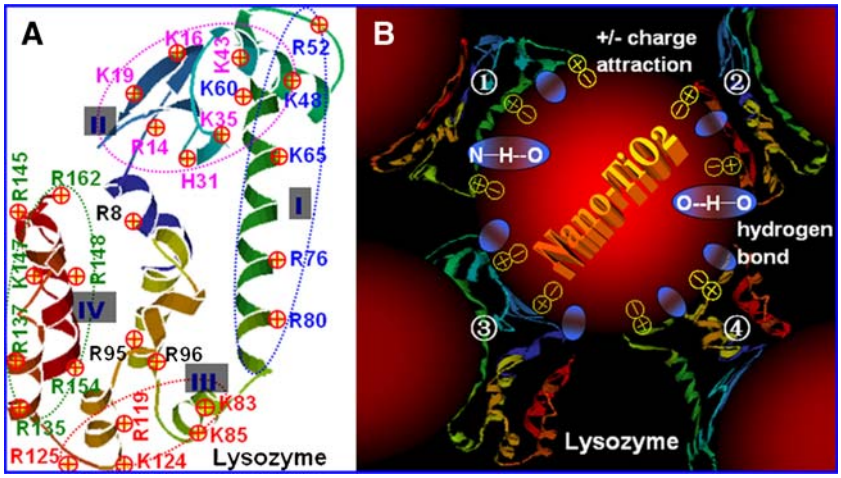

Fig. 5 **a** Lysozyme structure and distribution of the positively charged amino acid residues, which were divided into four areas from I to IV; **b** cartoon illustrating the possible binding sites of lysozyme on TiO_2 particle via N–H···O or O–H···O hydrogen bonds and positive–negative electrostatic attraction where four areas were collected on TiO_2 particle surface to cause deformation of the lysozyme spatial structure

hydrogen bond will form between TiO_2 and the polar side chains of amino acid residues (see Fig. 5b). Thus, the combination of noncovalent electrostatic interactions and hydrogen bonds led to the firm binding of lysozyme on TiO_2 particle. From the SEM image (see Fig. 3a) and size distribution of TiO_2-only particles (see Fig. 4b), the particles easily form into irregular, huge self-aggregates. After lysozyme is added, the TiO_2–lysozyme particles become colloidal and conjointly global from the independent regular globes (see Fig. 3). As well, their aggregates become bigger with increasing lysozyme from 0 to 1.39 μM (see Fig. 4b). For example, the particle numbers being more than 5 and 7 μm in size occupy only 11% and 0% in the absence of lysozyme from the column height, but over 25% and 50% in 1.39 μM lysozyme media, respectively. When lysozyme is more than 1.39 μM, e.g., the mass ratio of lysozyme to TiO_2 at 1.4, the particle mean size reaches a maximum at 5.5 μm from only 3.3 μm, i.e., lysozyme approaches an adsorption saturation and bridges between nano-TiO_2 particles (see Fig. 4b). This was confirmed from the above data (see Fig. 1c).

3.3 Effect of TiO_2 particle on the secondary structure of lysozyme

For the convenience of analyzing the interaction mechanism, lysozyme was divided into four areas from I to IV according to the distribution of the basic amino acid residues: R52, K48, K60, K65, R76, and Re80 in area I, K16, K19, R52, K43, K48, K35, H31, and R14 in area II, K83, K85, R119, K124, and R125 in area III, and R162, R145, R148, K147, R187, K135, R154, and R125 in area IV (see Fig. 5a) where only the side groups of both R and K residues are charged positively at pH 7.4. The positively charged side groups of each area may be collected together to bind onto the TiO_2 particle surface via ± electrostatic interaction (see Fig. 5b). When the lysozyme is close to the TiO_2 surface, many hydrogen bonds will be formed between TiO_2 and the polar side groups of lysozyme in the N–H···O and O–H···O types, e.g., E64, D61, D70, and D72 in area I, D47, E45, D20, and E22 in area II, D89 and D92 in area III, and D159 and E128 in area IV (see Fig. 5b). From a change of the particle shape from the regular TiO_2-only globe into the TiO_2–lysozyme colloid (see Fig. 3), some areas of lysozyme bridge between nano-TiO_2 particles to form bigger particles, e.g., areas I and IV of lysozymes 1 and 2, areas I and II of lysozyme 3, and areas II and III of lysozyme 4. Thus, a big particle aggregate was formed where many lysozyme molecules were clamped among nano-TiO_2 particles. Without doubt, the twist and deformation of the lysozyme spatial structure will occur under the traction of TiO_2 particles. The specific conformation of a protein with a particular function results from interactions among its amino acid residues. CD spectrometry is often used to characterize the secondary structure of a protein with β-pleated sheet, β-turn, α-helix,

Table 1 Determination of the lysozyme's secondary structure

Factor	Fraction(%)±SD			
	No TiO_2	5mg/L TiO_2	20mg/L TiO_2	40mg/L TiO_2
α-Helix	24.0±1.2	22.1±1.1	20.1±0.8	10.9±0.6
β-Sheet	37.8±2.1	46.7±2.4	51.9±1.9	64.4±3.0
β-Turn	6.2±0.3	3.1±0.12	0±0	0±0
Random coil	32.0±1.7	28.2±0.15	28.0±0.14	24.6±0.21

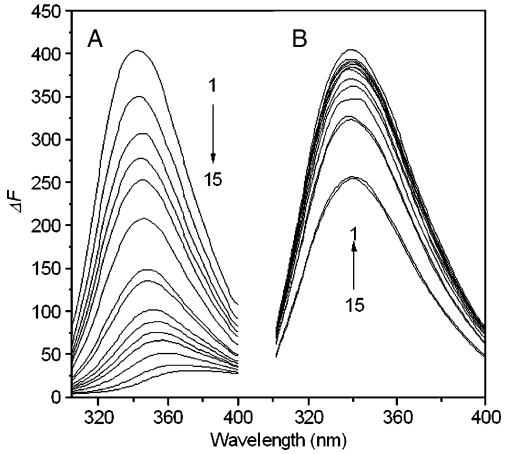

Fig. 6 **a** Fluorescence spectra of the nano-TiO_2–lysozyme suspensions containing 0.690 μM lysozyme and TiO_2 concentrations of 0, 2, 4, 6, 8, 10, 15, 20, 25, 30, 40, 50, 60, 80, and 100 mg/L (from curve *1* to *15*) at pH 7.4 in 0.15 M NaCl measured against the reagent blank; **b** those of the supernatants of the above suspensions

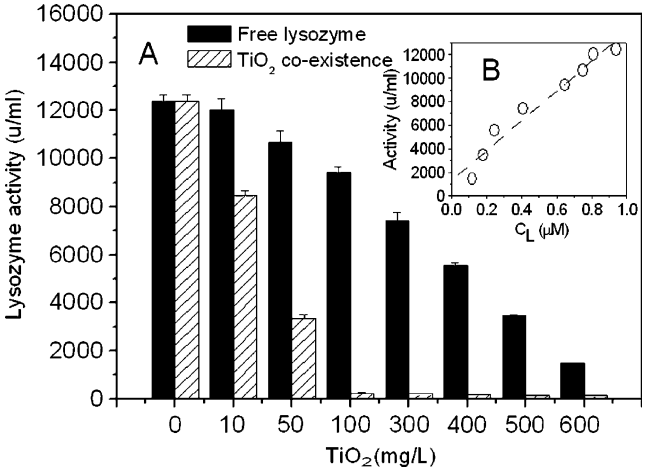

Fig. 8 **a** Variation of lysozyme activity in the presence of nano-TiO_2 where the suspensions contained 0.972 μM lysozyme and nano-TiO_2 from 0 to 600 mg/L at pH 7.4 in 0.15 M NaCl; **b** correlation between activity of the lysozyme free in the supernatants of the above suspensions and the lysozyme concentration (c_L) determined at 280 nm by UV spectrophotometry

and random coil. From CD change of the lysozyme in the presence of nano-TiO_2 particles (Fig. S2 of the Electronic supplementary material), the fractions of α-helix and β-turn decrease obviously with increasing TiO_2 particles but the β-pleated sheet increases (Table 1). For example, the α-helix decreases from 24% in the absence of TiO_2 down to 10.9% in 40 mg/L TiO_2 media, but the β-sheet increases from 37.8% up to 66.4%. Therefore, the effect of TiO_2 particles is obviously on the secondary structure of lysozyme. This is consistent with protein adsorption onto silica nanoparticles (Lundqvist et al. 2004), but contrasts with the binding of small organic substance in lysozyme (Chen et al. 2008). A possible reason is that lots of polar side groups of lysozyme bind onto TiO_2 particles to cause the twist and deformation of the lysozyme chain (see Fig. 5b) so that the inner hydrogen bonds of the helix are destroyed. β-Pleated sheet can induce the formation of amyloid fibrils, a process which plays a major role in pathology (Goto et al. 2008).

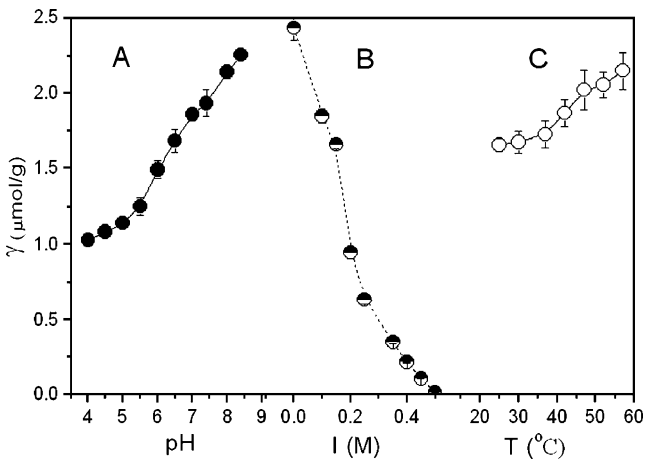

Fig. 7 Effects of pH, electrolyte, and temperature on γ of lysozyme. **a** pH from 4.0 to 8.4; **b** NaCl from 0 to 0.5 M at pH 7.4; and **c** temperature from 25°C to 57°C at pH 7.4. The suspensions initially contained 140 mg/L nano-TiO_2 and 0.972 μM lysozyme

3.4 Fluorescence analysis of the lysozyme–nano-TiO_2 interaction

In order to further investigate the interaction of lysozyme with nano-TiO_2 particles, the fluorescence spectra of the nano-TiO_2–lysozyme suspensions are determined (Fig. 6a). The fluorescence intensity of the liquid decreases sharply with increasing nano-TiO_2, but that of the free lysozyme decreased very slowly when measuring the supernatant (see Fig. 6b). The light scattering of suspending TiO_2 particles is obvious so that the fluorescence quenching of the suspension obviously occurs. For example, the fluorescence of free lysozyme changed by less than 10% in 20 mg/L nano-TiO_2 media, but the fluorescence intensity of the suspension decreases by 75%. When nano-TiO_2 is more than 45 mg/L, over 90% of the fluorescence of free lysozyme is scattered. An additional reason is that the side groups of tryptophan residues: W126, W138, and W158 located in area IV (see Fig. 5a) may bind to TiO_2 particles via the N–H···O hydrogen bonds owing to the twist and deformation of lysozyme on TiO_2 particles. A red shift of the emission peak appears in Fig. 6a, but the same phenomenon is not observed in Fig. 6b. It is attributed to the fact that TiO_2 particles have a stronger light absorption or scattering at a short wavelength than that at a long wavelength. Moreover, the presence of nano-TiO_2 particles has not affected the conformation of lysozyme free in the suspension.

3.5 Effect of pH, ionic strength, and temperature

The effects of pH, electrolyte content, and temperature on the interaction of lysozyme with nano-TiO_2 particles are shown in Fig. 7. Curve A shows that γ increases with increasing pH from 4.0 to 8.4. From the isoelectric point of lysozyme at pH 6.0, the negative charges on the TiO_2 particle surface were neutralized in a more acidic media so that the electrostatic interaction weakened and the adsorption of lysozyme decreased. It is in agreement with the interaction of BSA with nano-TiO_2 particles (Giacomelli et al. 1997). From curve B, γ decreases with increasing ionic strength from 0 to 0.5 M. This is different from the adsorption behavior between protein and nano-TiO_2 reported by Oliva et al. (2003). The surface double electric layer of nano-TiO_2 particles will adsorb plenty of Na^+ to result in a repulsion of the positively charged side groups of lysozyme. The induction, orientation, and dispersion forces between lysozyme and nano-TiO_2 become stronger in a highly salty media due to polarization. This demonstrated that the electrostatic attraction is the main interaction type in the lysozyme–TiO_2 suspension. Curve C shows that γ increases with increasing temperature. This is attributed to the fact that the molecular motion quickens and the lysozyme–TiO_2 aggregate may become smaller at a higher temperature.

3.6 Effect of nano-TiO_2 particles on the lysozyme activity

The structure of a protein corresponds with the function so that a structural variation may destroy the normal physiological action (Hu and Xu 1999). Lysozyme can attack a specific component of certain bacterial cell walls, such as the peptidoglycan composed of *N*-acetylglucosamine (NAG) and *N*-acetylmuramic acid (NAM) cross-linked by peptide bridges, by hydrolyzing the bond between NAG and NAM. This increases the permeability of the wall and causes lysis of the bacterium. Inevitably, the binding of any chemical substance with a protein or enzyme, particularly an organic compound, will affect the protein function or enzyme activity (Derham and Harding 2006; Liu et al. 2000). From the above data, effect of the nano-TiO_2 particles on lysozyme structure is obvious. The lysozyme activity was determined in nano-TiO_2 media and its change is shown in Fig. 8a. The activity of lysozyme is obviously inhibited with increasing nano-TiO_2 particles. For example, lysozyme approaches a complete inactivation (only 200 U/mL) in 100 mg/L TiO_2 media. However, the independent activity of lysozyme free in the suspension is more than 9,000 U/mL, a level which is quite high. From Fig. 8b, the activity of lysozyme free in the corresponding supernatant is in a direct ratio to the lysozyme concentration, i.e., the TiO_2 particle has not affected the independent activity of lysozyme. One reason is that the active cleft of the lysozyme binding onto nano-TiO_2 particles was covered. Thus, it is difficult for the bond between NAG and NAM of the peptidoglycan chain to insert into the active cleft (Wang et al. 2007; Sanderson et al. 2007; Simon et al. 2007). The other reason is that many nano-TiO_2 particles may aggregate on the bacteria to cover the bond between NAG and NAM of the peptidoglycan chain. Thus, the attack process of lysozyme was cut off. Both the simultaneous interactions led to the complete inactivation of lysozyme in the TiO_2 coexistence.

4 Conclusions

The adsorption of lysozyme obeyed the Langmuir isothermal model with approximately 580 of the saturation number and 4.7×10^6 M^{-1} of the stability constant. The acidity and ion strength of media affected the binding of lysozyme. The bigger TiO_2 aggregate was formed in the presence of lysozyme where lysozyme may bridge between nano-TiO_2 particles. The coexistence of nano-TiO_2 particles resulted in a transition of the lysozyme conformation from α-helix into β-sheet and an obvious inactivation of lysozyme. The β-sheet can induce the formation of amyloid fibrils, a process which plays a major role in pathology.

5 Recommendations and perspectives

By investigating the interaction of nano-TiO_2 with lysozyme, the action sites and types are identified. The effect on the enzyme structure and activity is estimated and the toxicity mechanism of nano-TiO_2 is revealed. Our results strongly suggest that nano-TiO_2 has some impacts on enzyme. They indicate that nano-TiO_2 might have impacts on natural immunity. And more attention should be paid to the potential toxicity of nanomaterials on biomolecules. There are potentially multiple effects of nano-TiO_2, and the possible adverse effects of nano-TiO_2 exposure need further clarification. Further research into the toxicity of nanosized particles needs to be carried out prior to their causing cell and tissue toxicity. These investigations might serve as the basis for the toxicity and application of nanomaterials.

Acknowledgements This work was supported by the National Major Project of Science and Technology Ministry of China (no. 2008ZX07421-002) and the State Key Laboratory Foundation of Science and Technology Ministry of China (grant no. PCRRK08003).

References

Buzea C, Pacheco I, Robbie K (2006) Nanomaterials—sources, classification, and toxicity. Comp Biochem Physiol A 143(4): S123–S123

Chen FF, Tang YN, Wang SL, Gao HW (2008) Binding of brilliant red compound to lysozyme: insights into the enzyme toxicity of water-soluble aromatic chemicals. Amino Acids 36(3):399–407

Chen XH, Zhang L, Weng YX, Du LC, Ye MP, Yang GZ, Fujii R, Rondonuwu FS, Koyama Y, Wu YS, Zhang JP (2005) Protein structural deformation induced lifetime shortening of photosynthetic bacteria light-harvesting complex LH2 excited state. Biophys J 88(6):4262–4273

Chen YL, Zhang XF, Gong YD, Zhao NM, Zeng TY, Song XQ (1999) Conformational changes of fibrinogen adsorption onto hydroxyapatite and titanium oxide nanoparticles. J Colloid Interface Sci 214(1):38–45

Derham BK, Harding JJ (2006) The effect of the presence of globular proteins and elongated polymers on enzyme activity. Biochim Biophys Acta 1764(6):1000–1006

Donaldson K, Stone V, Seaton A, MacNee W (2001) Ambient particle inhalation and the cardiovascular system: potential mechanisms. Environ Health Perspect 109:523–527

Dunford R, Salinaro A, Cai LZ, Serpone N, Horikoshi S, Hidaka H, Knowland J (1997) Chemical oxidation and DNA damage catalysed by inorganic sunscreen ingredients. FEBS Lett 418 (1–2):87–90

Fenech M (2000) The in vitro micronucleus technique. Mutat Res 455 (1–2):81–95

Gao HW (1999) Establishment of SS absorption in suspension liquid. Asian J Chem 11(4):1556–1558

Gao HW, Zhao JF, Yang QZ, Liu XH, Chen L, Pan LT (2006) Non-covalent interaction of 2′,4′,5′,7′-tetrabromo-4,5,6,7-tetrachlorofluorescein with proteins and its application. Proteomics 6(19):5140–5151

Gao HW, Xu Q, Chen L, Wang SL, Wang Y, Wu LL, Yuan Y (2008) Potential protein toxicity of synthetic pigments: binding of poncean S to human serum albumin. Biophys J 94(3):906–917

Giacomelli CE, Avena MJ, DePauli CP (1997) Adsorption of bovine serum albumin onto TiO_2 particles. J Colloid Interface Sci 188 (2):387–395

Goto Y, Yagi H, Yamaguchi K, Chatani E, Ban T (2008) Structure, formation and propagation of amyloid fibrils. Curr Pharm Des 14 (30):3205–3218

Heinlaan M, Ivask A, Blinova I, Dubourguier HC, Kahru A (2008) Toxicity of nanosized and bulk ZnO, CuO and TiO_2 to bacteria *Vibrio fischeri* and crustaceans *Daphnia magna* and *Thamnocephalus platyurus*. Chemosphere 71(7):1308–1316

Hu HY, Xu GJ (1999) Structural transformation of proteins. Prog Biochem Biophys 26(1):9–12

Hund-Rinke K, Simon M (2006) Ecotoxic effect of photocatalytic active nanoparticles TiO_2 on algae and daphnids. Environ Sci Pollut Res 13(4):225–232

Lee YC, Yang D (2002) Determination of lysozyme activities in a microplate format. Anal Biochem 310(2):223–224

Li L, Gao HW, Ren JR, Chen L, Li YC, Zhao JF, Zhao HP, Yuan Y (2007) Binding of Sudan II and IV to lecithin liposomes and *E. coli* membranes: insights into the toxicity of hydrophobic azo dyes. BMC Struct Biol 7:6

Liu HS, Wang YC, Chen WY (1995) The sorption of lysozyme and ribonuclease onto ferromagnetic nickel powder 1. Adsorption of single components. Colloids Surf B 5(1–2):25–34

Liu ST, Sugimoto T, Azakami H, Kato A (2000) Lipophilization of lysozyme by short and middle chain fatty acids. J Agric Food Chem 48(2):265–269

Lovern SB, Strickler JR, Klaper R (2007) Behavioral and physiological changes in daphnia magna when exposed to nanoparticle suspensions (titanium dioxide, nano-C_{60}, and $C_{60}HxC_{70}Hx$). Environ Sci Technol 41(12):4465–4470

Lu NH, Zhu ZN, Zhao XQ, Tao R, Yang XL, Gao ZH (2008) Nano titanium dioxide photocatalytic protein tyrosine nitration: a potential hazard of TiO_2 on skin. Biochem Biophys Res Commun 370(4):675–680

Lundqvist M, Sethson I, Jonsson BH (2004) Protein adsorption onto silica nanoparticles: conformational changes depend on the particles' curvature and the protein stability. Langmuir 20 (24):10639–10647

Merlini G, Bellotti V (2005) Lysozyme: a paradigmatic molecule for the investigation of protein structure, function and misfolding. Clin Chim Acta 357(2):168–172

Oliva FY, Avalle LB, Camara OR, De Pauli CP (2003) Adsorption of human serum albumin (HSA) onto colloidal TiO_2 particles, part I. J Colloid Interface Sci 261(2):299–311

Roddick-Lanzilotta AD, Connor PA, McQuillan AJ (1998) An in situ infrared spectroscopic study of the adsorption of lysine to TiO_2 from an aqueous solution. Langmuir 14(22):6479–6484

Sanderson BJS, Wang JJ, Wang H (2007) Letter and new data in response to Letter to the Editor by William P. Gulledge about article "Cyto- and genotoxicity of ultrafine TiO_2 particles in cultured human lymphoblastoid cells" by Wang et al. Reply. Mutat Res 634(1–2):243–244

Sela MN, Badihi L, Rosen G, Steinberg D, Kohavi D (2007) Adsorption of human plasma proteins to modified titanium surfaces. Clin Oral Implants Res 18(5):630–638

Simon A, Gouget B, Mayne M, Herlin N, Reynaud C, Degrouard J, Carriere M (2007) In vitro investigation of TiO_2, Al_2O_3, Au nanoparticles and multi-walled carbon nanotubes cyto- and genotoxicity on lung, kidney cells and hepatocytes. Toxicol Lett 172:S36–S36

Stone V, Johnston H, Clift MJD (2007) Air pollution, ultrafine and nanoparticle toxicology: cellular and molecular interactions. IEEE Transactions on NanoBioscience 6(4):331–340

Turkan Kopac KB, Yener J (2008) Effect of pH and temperature on the adsorption of bovine serum albumin onto titanium dioxide. Colloids Surf A Physicochem Eng Asp 322(2008):19–28

Van Dael H (1998) Chimeras of human lysozyme and alpha-lactalbumin: an interesting tool for studying partially folded states during protein folding. Cell Mol Life Sci 54(11):1217–1230

Voros J (2004) The density and refractive index of adsorbing protein layers. Biophys J 87(1):553–561

Wang JJ, Sanderson BJS, Wang H (2007) Cyto- and genotoxicity of ultrafine TiO_2 particles in cultured human lymphoblastoid cells. Mutat Res 628(2):99–106

Zhu MT, Feng WY, Wang B, Wang TC, Gu YQ, Wang M, Wang Y, Ouyang H, Zhao YL, Chai ZF (2008) Comparative study of pulmonary responses to nano- and submicron-sized ferric oxide in rats. Toxicology 247(2–3):102–111